

Study of Heat Transfer Correlations for Supercritical Hydrogen in Regenerative Cooling Channels

Justin M. Locke* and D. Brian Landrum†

University of Alabama in Huntsville, Huntsville, Alabama 35899

DOI: 10.2514/1.22496

Understanding the cooling efficiency of supercritical hydrogen is crucial to the development of high-pressure thrust chambers for regeneratively cooled liquid-oxygen/liquid-hydrogen rocket engines. Available Nusselt number correlations are compared with an extensive data set of local heat transfer coefficients to determine the domains of validity for each correlation. The data set was compiled from previous heated straight-tube experiments with supercritical hydrogen. Results indicate that particular correlations perform better than others for certain regimes of fluid properties, with the accuracy of heat transfer coefficient predictions ranging from ± 23 to over $\pm 100\%$. Correlation uncertainty due to inherent uncertainties in the equation-of-state and transport properties of supercritical hydrogen is also evaluated. The property dependent uncertainty was found to range from 2 to 10%, and therefore is not the main contributor to the larger errors in the correlation predictions. A number of published correlations for nonhydrogen supercritical fluids are shown to achieve comparable performance with hydrogen.

Nomenclature

C_p	=	constant pressure specific heat, kJ/(kg · K)
D	=	inner diameter of tube, m
h	=	heat transfer coefficient, W/(m ² · K)
k	=	thermal conductivity, W/(m · K)
\dot{m}	=	mass flow rate, kg/s
Nu	=	Nusselt number
P	=	pressure, MPa
P_R	=	reduced pressure
Pr	=	Prandtl number
Re	=	Reynolds number
T	=	temperature, K
T^*	=	pseudocritical temperature, K
T_R	=	reduced temperature
U	=	uncertainty
V	=	velocity, m/s
x	=	distance downstream from entrance
x	=	any property
μ	=	dynamic viscosity, kg/(m · s)
ν	=	kinematic viscosity, m ² /s
ρ	=	density, kg/m ³
σ	=	standard deviation

Subscripts

b	=	property evaluated at bulk temperature reference
c	=	critical condition
calc	=	calculated value
exp	=	experimental value
f	=	property evaluated at film temperature reference
pc	=	pseudocritical
ref	=	reference temperature type
s	=	condition at inner-wall surface
\int	=	property evaluated by integral method

Introduction

ANALYTICAL performance predictions and design analyses for regeneratively cooled liquid rocket engines use correlations to predict the heat transfer from the combusting gas to the thrust chamber wall and from the wall into the cooling fluid. Today, these correlations are used in many engineering level computational analysis tools [1] for thrust chamber cooling system design, and cycle power-balance programs [2], which are increasingly being used in the design and evaluation of complete liquid rocket engine systems. In addition, these correlations are often used to aid the design of many of the experiments aimed at obtaining benchmark computational fluid dynamics data [3]. They are also used as validity checks of computational results. These semi-empirical heat transfer correlations are highly dependent on the fluid transport properties and the conditions at which the fluid is flowing [4–6]. Although a number of coolant-side correlations have been proposed for hydrogen [7–15], their ability to accurately predict heat transfer over a wide range of operating conditions has typically been limited.

Improved thrust chamber design requires accurate correlations for different geometries, such as high aspect ratio rectangular channels and curvature, as well as asymmetric heating and varying heat flux. For correction factors and new correlations to have any merit, it is important to understand the limitations of current correlations for the simplest case: a straight, uniformly heated, circular tube. This paper examines existing correlations for straight-tube geometries using supercritical hydrogen coolant. Previous experimental data are compared with existing published correlations over the supercritical property region to determine the domains of validity for each correlation. The contribution to correlation uncertainty due to inherent uncertainties in the equation-of-state and transport properties of supercritical hydrogen is also evaluated. Finally, a number of correlations for other supercritical fluids flowing turbulently in straight circular tubes are evaluated for use with supercritical hydrogen.

Background

In typical rocket applications, hydrogen enters the coolant channels as a liquid above the critical pressure ($P_c = 1.3$ MPa) and at temperatures as low as 25 K, which is well below the critical temperature ($T_c = 33$ K). High-pressure thrust chambers also operate with very high Reynolds number flow conditions ($Re > 10^6$) in the coolant passages [16]. As the hydrogen continues through the channels, it is quickly heated to above the critical temperature, where it becomes a supercritical gas (see Fig. 1). The heat transfer

Received 11 February 2006; revision received 26 April 2007; accepted for publication 21 May 2007. Copyright © 2007 by the authors. Published by the American Institute of Aeronautics and Astronautics, Inc., with permission. Copies of this paper may be made for personal or internal use, on condition that the copier pay the \$10.00 per-copy fee to the Copyright Clearance Center, Inc., 222 Rosewood Drive, Danvers, MA 01923; include the code 0748-4658/08 \$10.00 in correspondence with the CCC.

*Graduate Research Assistant, Propulsion Research Center, Department of Mechanical and Aerospace Engineering; jml511@psu.edu. Member AIAA.

†Associate Professor, Propulsion Research Center, Department of Mechanical and Aerospace Engineering; landrum@mae.uah.edu. Associate Fellow AIAA.

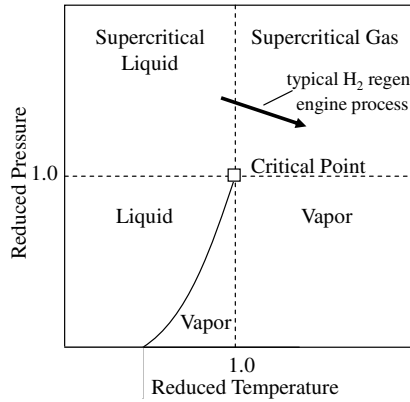


Fig. 1 Typical H₂ regenerative thrust chamber conditions with hydrogen as coolant.

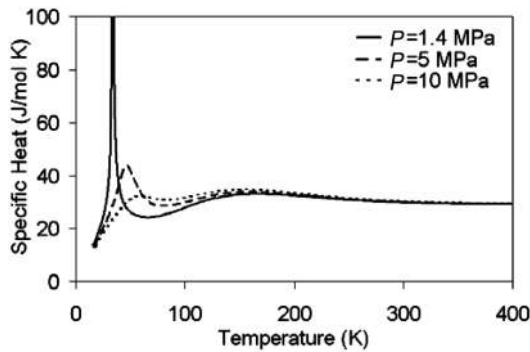


Fig. 2 Variation of hydrogen specific heat with pressure [30].

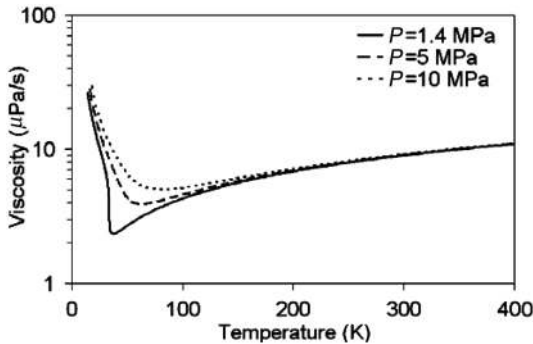


Fig. 3 Variation of hydrogen viscosity with pressure [30].

mechanisms occurring in these regions are supercritical liquid and supercritical gas forced convection [17].

Numerous experimental studies, most of which took place in the 1960s, have been performed for supercritical hydrogen flowing in uniformly heated circular tubes [7,9,16,18–24]. These studies produced Nusselt number correlations that are principally based on the conventional Dittus–Boelter equation for turbulent, thermally fully developed flow for fluids with constant property values [25],

$$Nu = 0.023Re^{0.8}Pr^{0.4} \quad (1)$$

where Re is the Reynolds number and Pr the Prandtl number. However, the properties of hydrogen vary considerably with temperature and pressure, as demonstrated in Figs. 2 and 3 for specific heat and viscosity. Density and thermal conductivity also vary with temperature and pressure. To account for these varying properties, either a change in reference conditions or additional terms are needed.

In 1960, McCarthy and Wolf proposed a modified version of the Dittus–Boelter equation [7],

$$Nu_b = 0.025Re_b^{0.8}Pr_b^{0.4}(T_s/T_b)^{-0.55} \quad (2)$$

where the subscript b denotes properties evaluated at the bulk temperature of the fluid and T_s/T_b is the inner-wall-to-bulk temperature ratio. In 1965, Hendricks et al. replaced the bulk condition and proposed the correlation [8],

$$Nu_f = 0.021Re_f^{0.8}Pr_f^{0.4} \quad (3)$$

where the properties are evaluated at the film temperature,

$$T_f = (T_s + T_b)/2 \quad (4)$$

Hess and Kunz, also in 1965, proposed a modified version of the film temperature-type correlation that included wall-to-bulk viscosity ratio [9],

$$Nu_f = 0.0208Re_f^{0.8}Pr_f^{0.4}(1 + 0.01457v_s/v_b) \quad (5)$$

Miller (1965) proposed using a new reference temperature and developed the correlation [10]

$$Nu_{0.4} = 0.0208(Re_{0.4})^{0.8}(Pr_{0.4})^{0.4}(1 + 0.00983v_s/v_b) \quad (6)$$

where

$$T_{0.4} = T_b + 0.4(T_s - T_b) \quad (7)$$

This approximately constant reference temperature is equivalent to Deissler's comprehensive theory which describes forced convective heat transfer for turbulent flow at supercritical gas conditions sufficiently above the critical temperature [17].

Taylor, working in 1968–1970 in support of the Nuclear Engine for Rocket Engine Advancement (NERVA) and Phoebus-2 nuclear rocket engine program, added a correction factor to the McCarthy and Wolf correlation to improve the heat transfer along the length of the tube [11–14],

$$Nu_b = 0.023Re_b^{0.8}Pr_b^{0.4}(T_s/T_b)^{-(0.57 - \frac{150}{x/D})} \quad (8)$$

The x/D factor was proposed to correct for the entrance effects observed during tests. In 1973, Schact and Quentmeyer proposed a new type of reference condition that uses an integral averaging of property x over the inner-wall-to-bulk temperature [15],

$$x = \frac{1}{T_s - T_b} \int_{T_b}^{T_s} x(T) dT \quad (9)$$

The resultant correlation is

$$Nu_f = 0.025Re_f^{0.8}Pr_f^{0.4} \quad (10)$$

References [25–27] provide a good summary of other turbulent flow forced convection correlations to fluids in circular ducts at supercritical pressures. Most of these were developed from experiments using H₂O and CO₂ as the fluids, and could potentially be adapted for use with hydrogen. In addition, by replacing the circular tube diameter with a hydraulic diameter, these correlations can also be applied to rectangular ducts and therefore high aspect ratio cooling channels [26].

Evaluation with Experimental Data

To assess the validity of available correlations, published experimental heat transfer data for hydrogen in the supercritical regime was gathered and reduced using current hydrogen property databases. Data from experiments conducted by Hendricks et al. (NASA Lewis, 1965) [8] and Hendricks et al. (NASA Lewis, 1966) [23], Aerojet-General Corporation (1967) [24], and McCarthy and Wolf (Rocketdyne Division, North American Aviation, 1960) [28] were used. The ranges of conditions tested in these experimental

Table 1 Summary of heat transfer experiments used in analysis

Investigator	ID, cm	x/D	T_s/T_b	T_b , K	P , MPa	Heat flux, MW/m ²	Mass flow rate, kg/s
Rocketdyne [28]	—	—	1.6–2.26	324–399	4.78–17.1	10.9–56.3	—
Hendricks et al. [8]	0.536–1.11	3.4–78.2	1.5–11.0	33–111	6.89–17.2	0.98–16.4	0.023–0.181
Hendricks et al. [23]	0.478–1.29	4.9–114	1.1–15	25–278	1.52–5.65	0.33–5.4	0.013–0.088
Aerojet [24]	0.376	6.7–33.9	6.1–21.4	34–54	4.80–9.45	10.5–45	0.032–0.200

Table 2 Performance of correlations based on predicted and experimental Nu for NASA Lewis, TN D-2977 dataset (870 data points)

Investigators	Percent of H ₂ data points within prescribed limits				Limits to cover 95% of H ₂ data
	±10%	±15%	±20%	±25%	
McCarthy and Wolf [7]	37	53	66	75	43
Hendricks et al. [8]	34	51	65	77	40
Hess and Kunz [9]	38	55	69	79	39
Miller [10]	41	57	68	78	37
Taylor [14]	42	59	73	86	33
Schact and Quentmeyer [15]	39	57	69	78	41

Table 3 Performance of correlations based on predicted and experimental Nu for NASA Lewis, TN D-3095 dataset (1701 data points)

Investigators	Percent of H ₂ data points within prescribed limits				Limits to cover 95% of H ₂ data
	±10%	±15%	±20%	±25%	
McCarthy and Wolf [7]	26	36	45	52	120
Hendricks et al. [8]	20	30	38	46	75
Hess and Kunz [9]	25	39	50	59	70
Miller [10]	24	36	47	57	71
Taylor [14]	27	38	46	54	111
Schact and Quentmeyer [15]	26	37	48	57	63

programs can be found in Table 1. These sources were selected because their data sets were readily available, and because together they represent a wide range of fluid property conditions. Combined, they represent a total of 2992 individual measurements of local Nu values.

To compare the correlation predictions with the experimental data, the calculated heat transfer coefficient h_{calc} is determined by the relation

$$h_{\text{calc}} = \frac{Nu_{\text{calc ref}} k_{\text{ref}}}{D} \quad (11)$$

where $Nu_{\text{calc ref}}$ is determined using the various heat transfer correlations, Eqs. (2), (3), (5), (6), (8), and (10), k_{ref} is the thermal conductivity evaluated at the reference temperature, and D is the inner diameter of the tube. The reference Reynolds and Prandtl numbers used in the correlations are defined as

$$Re_{\text{ref}} = \frac{\rho_{\text{ref}} V_b D}{\mu_{\text{ref}}} = \frac{4\dot{m}}{\pi D \mu_{\text{ref}}} \frac{\rho_{\text{ref}}}{\rho_b} \quad (12)$$

and

$$Pr_{\text{ref}} = \frac{Cp_{\text{ref}} \mu_{\text{ref}}}{k_{\text{ref}}} \quad (13)$$

Here, \dot{m} is the mass flow rate, V_b and ρ_b are the bulk velocity and density, and ρ_{ref} , μ_{ref} , and Cp_{ref} are the density, thermal conductivity, and specific heat, evaluated at the reference temperature. The experimental heat transfer coefficient h_{exp} was calculated by the individual investigators at each measurement point. The percent deviation of predicted results to the experimental data is calculated by

$$\left(\frac{h_{\text{calc}}}{h_{\text{exp}}} - 1 \right) 100 = \text{Percent Deviation} \quad (14)$$

Property values for hydrogen were obtained from the National Institute of Standards and Technology (NIST) *Thermodynamic and Transport Properties of Pure Fluids* database [29] and the NIST *Chemistry WebBook* [30]. These sources are based on [31] for density and specific heat, and [32] for viscosity and thermal conductivity. They contain data for temperatures up to 400 K. For conditions above 400 K, *Selected Property of Hydrogen (Engineering Design)* [33] was used, which is an updated version of [34], to correct for errors in certain property data.

The accuracy of experimental heated tube data is generally reported by considering a heat balance. The power input is checked against the enthalpy increase of the hydrogen, which is calculated from the flow rate, inlet and outlet bulk temperatures, and the hydrogen transport properties. For the data sets considered in this study, Hendricks et al. (NASA TN D-2977) [8] report a heat balance of generally less than ±8%; Hendricks et al. (NASA TN D-3095) [23] report heat balances for most runs within ±10%, with some runs on the order of ±20%; and McCarthy and Wolf (Rocketdyne [28]) [28] report an average heat balance of 5.9%, with most runs within ±10%. The Aerojet-General Corporation (1967) [24] study does not provide a quantitative assessment of heat balance accuracy for its straight-tube data. The heat balances were not recalculated in this paper in light of the newer transport property sets detailed earlier. All data sets were screened to rule out buoyancy effects, using the criteria provided in [27].

Existing Supercritical H₂ Correlations

Individual Data Sets

Tables 2–5 show the percent of experimental hydrogen data points that fall within various ranges of deviation (±10 to ±25%) from the correlations, as well as the range of correlation variation needed to cover 95% (or 2σ) of the data points. For the NASA Lewis TN D-2977 [8] data set, the 2σ range varied from ±33% for the Taylor correlation to ±43% for the McCarthy and Wolf correlation. The Taylor correlation predicted 86% of the data points to within ±25%.

Table 4 Performance of correlations based on predicted and experimental Nu for Aerojet dataset [24] (252 data points)

Investigators	Percent of H_2 data points within prescribed limits				Limits to cover 95% of H_2 data
	$\pm 10\%$	$\pm 15\%$	$\pm 20\%$	$\pm 25\%$	
McCarthy and Wolf [7]	26	40	54	62	43
Hendricks et al. [8]	0	0	0	5	55
Hess and Kunz [9]	27	40	63	71	46
Miller [10]	35	49	65	76	44
Taylor [14]	60	81	88	94	26
Schact and Quentmeyer [15]	47	62	74	85	33

Table 5 Performance of correlations based on predicted and experimental Nu for Rocketdyne [28] dataset (168 data points)

Investigators	Percent of H_2 data points within prescribed limits				Limits to cover 95% of H_2 data
	$\pm 10\%$	$\pm 15\%$	$\pm 20\%$	$\pm 25\%$	
McCarthy and Wolf [7]	52	65	76	90	28
Hendricks et al. [8]	50	69	85	98	23
Hess and Kunz [9]	54	63	73	83	47
Miller [10]	55	64	73	79	49
Taylor [14]	52	64	74	86	44
Schact and Quentmeyer [15]	45	66	76	76	52

Table 6 Performance of correlations based on predicted and experimental Nu for all four datasets combined (2992 data points)

Investigators	Percent of H_2 data points within prescribed limits				Limits to cover 95% of H_2 data
	$\pm 10\%$	$\pm 15\%$	$\pm 20\%$	$\pm 25\%$	
McCarthy and Wolf [7]	31	43	54	62	86
Hendricks et al. [8]	24	36	45	54	68
Hess and Kunz [9]	31	45	58	67	62
Miller [10]	32	45	56	66	62
Taylor [14]	36	49	59	68	78
Schact and Quentmeyer [15]	33	46	58	66	56

For the NASA Lewis TN D-3095 [23] data set, the 2σ range varied from $\pm 63\%$ for the Schact and Quentmeyer correlation to $\pm 120\%$ for the McCarthy and Wolf correlation. The Schact and Quentmeyer correlation predicted 54% of the data to within $\pm 25\%$.

For the Aerojet [24] data set, the 2σ range varied from $\pm 26\%$ for the Taylor correlation to $\pm 55\%$ for the Hendricks correlation. The Taylor correlation predicted 94% of the data points to within $\pm 25\%$. Finally, for the Rocketdyne data set, the 2σ range varied from $\pm 23\%$ for the Hendricks correlation, with 98% coverage at $\pm 25\%$, to 52% for the Schact and Quentmeyer correlation.

From these results, it cannot be ascertained that a particular correlation performs better than any other. In fact, although the Taylor correlation performs best for two of the data sets, it does not perform well for the NASA Lewis TN D-2977 [8] data set, with a 2σ range of $\pm 111\%$. Likewise, the Hendricks correlation predicts 98% of the Rocketdyne data to within $\pm 25\%$, but only 5% for the Aerojet data [24]. These differences are likely a result of the different fluid regions covered by each data set.

Combined Data Sets

Table 6 shows the percent of experimental hydrogen data points within prescribed correlation deviation limits, as well as the range to cover 95% of the data points, for all four data sets combined. It can be seen that the Schact and Quentmeyer correlation provides the best overall match with the experimental results, with a range of $\pm 56\%$ to cover 95% of the data. The results for the Taylor correlation show that it contains the most data points, 36% of the total number, within the prescribed limit of $\pm 10\%$ between predicted and experimental Nu values, and 68% for the limit of $\pm 25\%$. As a representative case, Fig. 4 shows the combined experimental data and the McCarthy and

Wolf correlation, plotted as reduced Nu vs the reference Reynolds number.

To better visualize the fluid conditions where the largest deviations are occurring, Fig. 5 shows the percent deviation of correlation predicted to experimental heat transfer coefficients, calculated by Eq. (14), on reduced temperature and pressure charts, calculated by Eq. (14) for each of the correlations. The Rocketdyne data, which are at higher reduced temperature, are not shown in Fig. 5 to afford clarity to the other three data sets. The McCarthy and Wolf [7] (Fig. 5a) and Taylor [14] (Fig. 5b) correlations (both bulk reference temperature types) overpredict the heat transfer in the region close to the critical point. These two correlations also overpredict along the pseudocritical temperature line T^* , which connects the peak values of specific heat. The Hendricks et al. [8] (Fig. 5b) correlation underpredicts along the pseudocritical temperature line and to the left, and also significantly underpredicts well above the T^* line. The Hess and Kunz [9] (Fig. 5d), Miller [10]

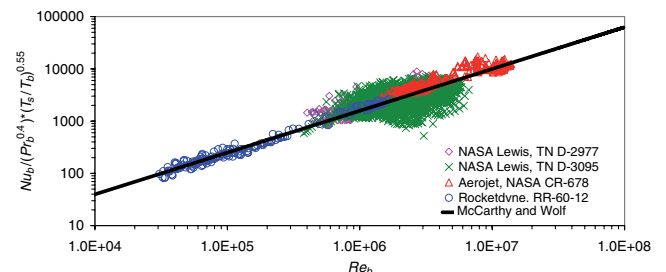


Fig. 4 Comparison of experimental Nu data with reduced McCarthy and Wolf correlation.

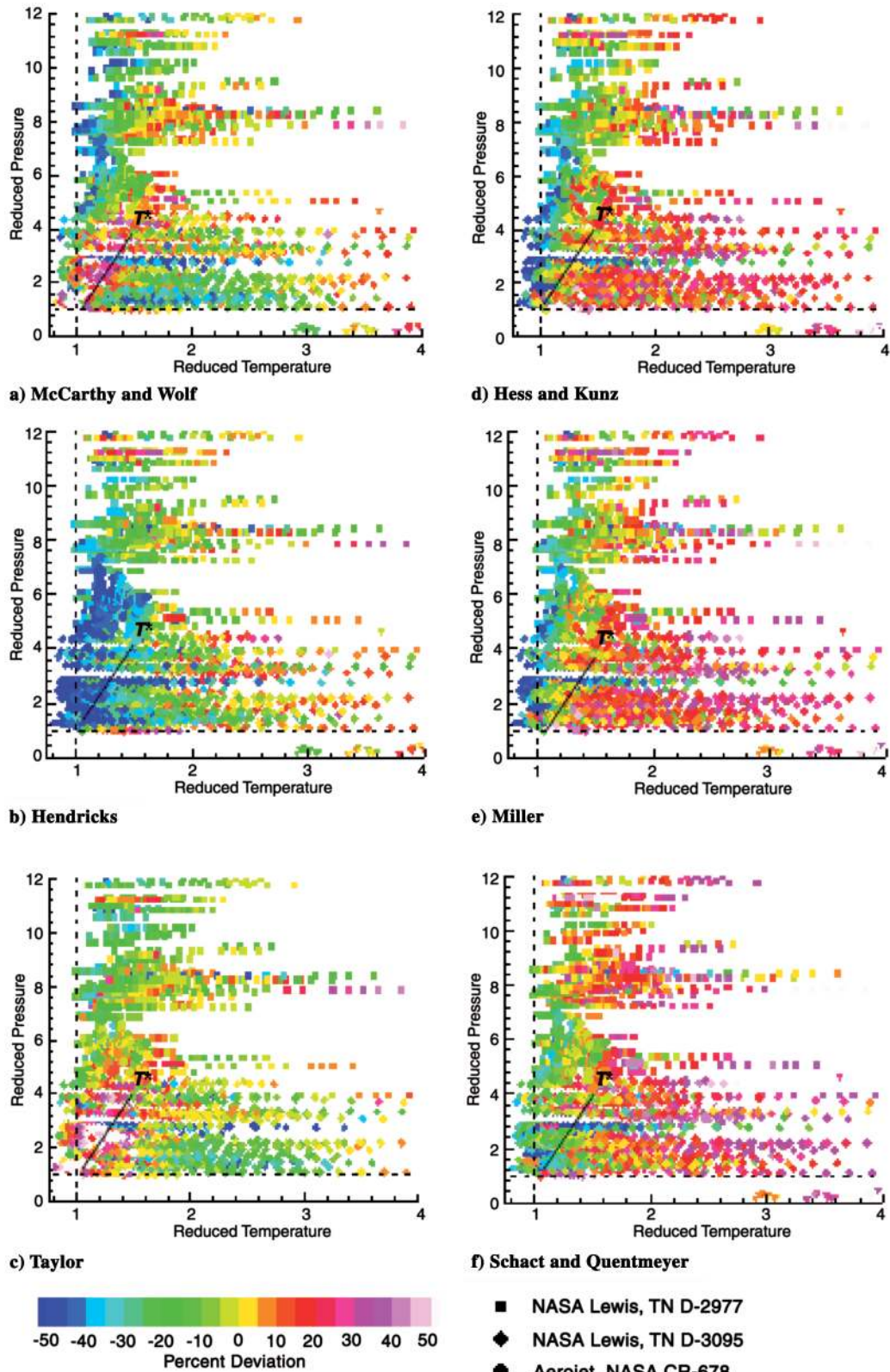


Fig. 5 Percent deviation of calculated to experimental heat transfer coefficients.

(Fig. 5e), and Schact and Quentmeyer [15] (Fig. 5f) correlations predict well along the T^* line. However, they all underpredict to various degrees to the left of this line. This may be a result of the flow not being thermally fully developed at the small x/D values of the experiments.

Comparing these plots to the purely analytical comparison of the correlations shown in Fig. 6, the difference in predictions between

the bulk-type correlations and the others is readily apparent. As can be seen in Fig. 6a for $Pr = 1.6$, both the McCarthy and Wolf and the Taylor correlations show a spike near the transition from liquid to supercritical gas ($T_R = 1$) line. This spike is a result of the peak in C_p that occurs here (corresponding to T^*). Given the deviations of the McCarthy and Wolf and Taylor correlations to the experimental results shown in Fig. 5, it is likely that this spike is actually an

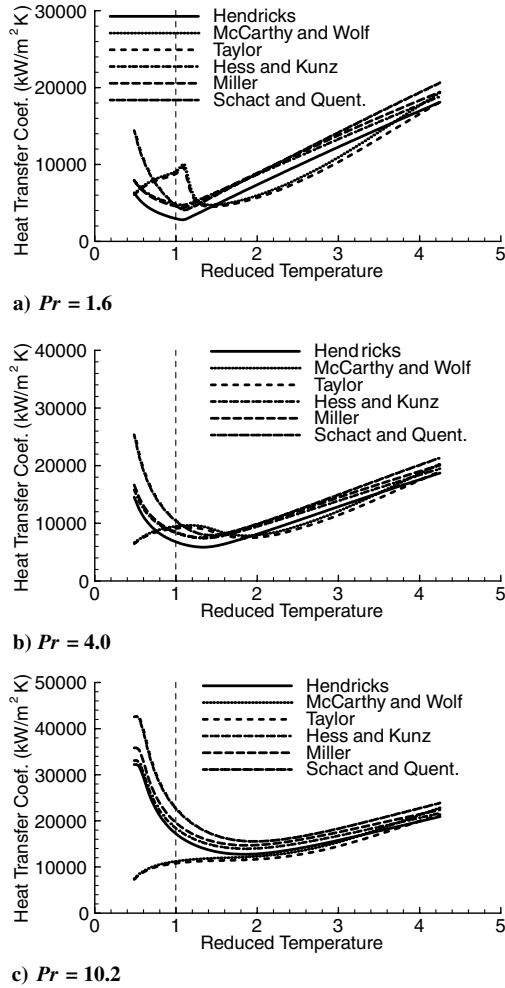


Fig. 6 Comparison of correlation predicted heat transfer coefficient of correlations for various reduced pressures ($Re_b = 2e6$, $T_s = 300$ K, $D = 0.01$ m, $x/D = 40$).

overprediction in this region and does not represent the true heat transfer. However, this is difficult to say conclusively due to the small x/D values for these experimental data where the flow may not be thermally fully developed.

Also from Fig. 5, it can be seen that the McCarthy and Wolf, Hendricks, Hess and Kunz, and Miller correlations underpredict in the region of the transition from liquid to supercritical gas for $P_R > 4$. As the pressure is increased, the range of underprediction for the McCarthy and Wolf correlation extends to larger temperature values up to about $T_R = 2$. This can be seen in Figs. 6b and 6c where the McCarthy and Wolf and Taylor correlations predict lower heat transfer coefficients than the other correlations at low temperatures. This divergence increases for lower temperatures and higher pressures. From Fig. 5, the Schacht and Quentmeyer correlation appears to give the most accurate prediction close to the $T_R = 1$ line for $P_R < 10$.

Reduced Regions

To assess the correlation predictions outside the transition from liquid to supercritical gas region, the range for 95% coverage of the experimental data was recalculated for $T_b \geq 50$ K. These results are shown in Table 7. It can be seen that the overall predictions for the combined data in this region are on the order of $\pm 40\%$, with little difference between correlations.

To eliminate some of the deviations that could be a result of entrance effects, Table 8 shows the ranges for 95% coverage considering only the data for $x/D \geq 20$. Here, the ranges for 95% coverage of the data for the combined data sets go from a minimum of $\pm 49\%$ for the Schacht and Quentmeyer correlation, to a maximum of over $\pm 100\%$ for the McCarthy and Wolf and Taylor correlations. Although $x/D \geq 20$ does not guarantee the flow is thermally fully developed, this does suggest that the poor predictions of the bulk reference-type correlations around the T^* line and the transition from liquid to supercritical gas are valid concerns if these correlations are used in these regions.

Correlations for Other Supercritical Fluids

A number of correlations have been published for other supercritical fluids, such as H_2O , CO_2 , and O_2 flowing turbulently in circular tubes [25–27,35]. As an attempt to find better correlations to predict the hydrogen heat transfer data examined in this current study, a number of these correlations were evaluated for their potential with supercritical hydrogen. The correlations and their comparison to hydrogen data are shown in Table 9.

The alternate correlations perform fairly well for the hydrogen data over the reduced region indicated. In particular, the McAdams [26] correlation predicted 83% of the hydrogen data to within $\pm 25\%$, with a range of $\pm 39\%$ from the correlations to cover 95% of the data. The Colburn [35] correlation predicted 80% of the hydrogen data to within $\pm 25\%$, with a range of $\pm 37\%$ from the correlations to cover 95% of the data. The Rohsenow [27] correlation predicted 73% of the hydrogen data to within $\pm 25\%$, with a range of $\pm 45\%$ from the correlations to cover 95% of the data. However, even the best matching correlations here do not provide any significant improvement over existing H_2 correlations.

Property Uncertainty Analysis

When conducting any experiment, the measurements of all variables have uncertainties associated with them, as do the values of fluid properties that are obtained through reference databases. These uncertainties propagate throughout the data reduction equation and produce an overall uncertainty for the calculated result [36]. For the case of this heat transfer analysis, the data reduction equations considered are the correlations from McCarthy and Wolf, Hendricks, Hess and Kunz, Miller, and Taylor [Eqs. (2), (3), (5), (6), and (8)], with the reference Reynolds and Prandtl numbers given by Eqs. (12) and (13), respectively.

The uncertainties listed in Table 10 are compiled from those quoted by the referenced sources and are based on accuracies of experimental measurements and inaccuracies introduced in fitting the data. No uncertainties are quoted in the near critical region, where they are expected to be considerably higher, but are not known quantitatively. Indeed, even an analytical function such as the

Table 7 Performance of correlations based on predicted and experimental Nu for all four datasets combined, for $T_b \geq 50$ K, $P > 1.284$ MPa only (1207 data points)

Investigators	Percent of H_2 data points within prescribed limits				Limits to cover 95% of H_2 data
	$\pm 10\%$	$\pm 15\%$	$\pm 20\%$	$\pm 25\%$	
McCarthy and Wolf [7]	45	61	74	83	40
Hendricks et al. [8]	43	61	73	83	40
Hess and Kunz [9]	42	61	74	84	40
Miller [10]	33	46	60	72	42
Taylor [14]	48	63	73	83	40
Schacht and Quentmeyer [15]	27	41	55	65	45

Table 8 Performance of correlations based on predicted and experimental Nu for all four datasets combined, for $x/D \geq 20$ (1991 data points)

Investigators	Percent of H_2 data points within prescribed limits				Limits to cover 95% of H_2 data
	$\pm 10\%$	$\pm 15\%$	$\pm 20\%$	$\pm 25\%$	
McCarthy and Wolf [7]	35	48	59	65	110
Hendricks et al. [8]	31	46	56	66	58
Hess and Kunz [9]	35	51	65	74	51
Miller [10]	35	49	61	71	50
Taylor [14]	36	48	58	66	100
Schact and Quentmeyer [15]	31	44	56	65	49

Table 9 Performance of correlations for non- H_2 fluids, evaluated for all four H_2 datasets combined, for $T_b \geq 50$ K, $P > 1.284$ MPa only (1207 data points)

Correlation	Investigators (fluids)	Percent of H_2 data points within prescribed limits				Limits to cover 95% of H_2 data
		$\pm 10\%$	$\pm 15\%$	$\pm 20\%$	$\pm 25\%$	
$Nu_b = 0.0214 Re_f^{0.8} Pr_f^{0.4} (k_f/k_b)[1 + 2.3/(x/D)]$	McAdams et al. [26], H_2O	43	61	73	83	39
$Nu_b = 0.023 Re_f^{0.8} Pr_f^{0.4} (k_f/k_b)(\rho_f/\rho_b)^{0.8}$	Powell [26], O_2	0	2.4	4	6	83
$Nu_b = 0.0266 Re_{ref}^{0.77} Pr_s^{0.55} (k_{ref}/k_b)(\rho_{ref}/\rho_b)^{0.77}$ where $T_{ref} = \begin{cases} T_b & \text{for } T_b < T_s < T_{pc} \\ T_{pc} & \text{for } T_b < T_s < T_{pc} \\ T_s & \text{for } T_b < T_s < T_{pc} \end{cases}$	Bringer and Smith [26], CO_2	5	7	8	9	94
$Nu_b = 0.023 Re_b^{0.8} Pr_{min}^{0.8}$ where $Pr_{min} = \min(Pr_b \text{ or } Pr_s)$	Miropolsky and Shitsman [26], CO_2, H_2O	6	11	14	20	123
$Nu_b = \begin{cases} Nu_{cp}(\mu_w/\mu_b)^{-0.11} & \text{for } T_b < T_s < T_{pc} \\ Nu_{cp}(\mu_w/\mu_b)^{-1} (k_w/k_b)(\bar{c}_p/c_{p,b})^{0.35} & \text{for } T_b < T_{pc} < T_s \text{ where } Nu_{cp} = \\ Nu_{cp}(\mu_w/\mu_b)^{-1} (k_w/k_b)^{0.66} (\bar{c}_p/c_{p,b})^{0.35} & \text{for } T_{pc} < T_b < T_s \end{cases}$ $(f/2) Re_b Pr_b / [12.7(f/2)^{1/2} (Pr_b^{2/3} - 1) + 1.07]$ and $f = 1/(3.64 \ln Re_b - 3.28)^2$	Kransoshchekov and Protopopov [26], CO_2, H_2O	12	19	27	34	72
$Nu_b = Nu_{cp}(\mu_w/\mu_b)^{-0.11} (k_w/k_b)^{0.33} (\bar{c}_p/c_{p,b})^{0.35}$	Petukhov et al. [26], CO_2, H_2O	1	2	4	6	75
$Nu_f = 0.10 Re_f^{0.66} Pr_f^{1.2}$	Domin [26], H_2O	0	0	1	4	63
$Nu_b = 0.00069 \bar{Pr}_b^{0.66} (\rho_w/\rho_b)^{0.43} [1 + 2.4/(x/D)]$ where $\bar{Pr}_b = \mu_b \bar{c}_p/k_b$	Bishop et al. [26], H_2O	10	16	24	32	67
$Nu_s = 0.00459 Re_s^{0.923} \bar{Pr}_s^{0.613} (\rho_s/\rho_b)^{0.231} (k_s/k_b)$ where $\bar{Pr}_s = \mu_s \bar{c}_p/k_s$	Swenson et al. [26], H_2O	22	35	46	57	63
$Nu_b = Nu_{cp}(\rho_s/\rho_b)^{0.3} (\bar{c}_p/c_{p,b})^n$ where $n = \begin{cases} 0.4 & \text{for } 1.2T_{pc} < T_b \\ 0.4 + 0.2[(T_s/T_{pc}) - 1] & \text{for } T_b < T_{pc} \\ 0.4 + 0.2[(T_s/T_{pc}) - 1]\{1 - 5[(T_b/T_{pc}) - 1]\} & \text{for } T_{pc} < T_b < 1.2T_{pc} \end{cases}$	Kransoshchekov and Protopopov-2 [26], CO_2, H_2O	0	0	0	0	84
$Nu_f = 6.3 + \frac{0.079(f)^{0.5} Re_f Pr_f}{(1 + Pr_f^{0.8})^{5/6}}$ where $(f)^{0.5} = \frac{1}{2.21 \ln(Re_f/7)}$	Churchill [25]	5	9	12	16	115
$Nu_b = 0.019 Re_b^{0.8} Pr_b^{0.4}$	Rohsenow [27]	31	47	62	73	45
$Nu_b = 0.0266 Re_b^{0.77} Pr_s^{0.55} (k_{ref}/k_b)(\rho_{ref}/\rho_b)^{0.77}$ where $T_{ref} = \begin{cases} T_{pc} & \text{for } 0.025 < (T_{pc} - T_b)/(T_s - T_b) < 0.30 \\ 0.10(T_s - T_b) - 3.0(T_{pc} - T_b) + T_b & \text{for } 0 < (T_{pc} - T_b)/(T_s - T_b) < 0.025 \end{cases}$	Schnurr [26], CO_2	15	22	28	34	148
$Nu_b = 0.0135 Re_b^{0.85} Pr_b^{0.8} F_c$ where $F_c = \begin{cases} 0.67 Pr_{pc}^{-0.05} (\bar{C}_p/C_{p,b})^{-0.77(1+1/Pr_{pc})+1.49} & \text{for } T_b < T_{pc} \\ (\bar{C}_p/C_{p,b})^{1.44(1+1/Pr_{pc})-0.53} & \text{for } T_{pc} < T_b \end{cases}$	Yamagata et al.-2 [26], H_2O	3	5	7	9	208
$Nu_b = 0.023 Re_b^{0.8} Pr_b^{1/3} (\frac{\mu_b}{\mu_w})^{0.14}$	Sieder and Tate [35]	4	5	7	9	163
$Nu_b = 0.023 Re_b^{0.8} Pr_b^{1/3}$	Colburn [35]	39	57	70	80	41
$Nu_f = 0.036 Re_f^{0.8} Pr_f^{1/3} (x/D)^{0.055}$	Nusselt [25]	9	15	22	31	70
$Nu_f = \frac{(f/2)(Re_f^{1000}) Pr_f}{1 + 12.7(f/2)^{0.5} (Pr_f^{2/3} - 1)}$ where $f = (1.58 \ln Re_f - 3.28)^{-2}$	Gnielinski [25]	26	40	56	69	47
$Nu_b = 0.023 Re_b^{0.8} Pr_{min}^{0.8} (\rho_s/\rho_b)^{0.3}$ where $Pr_{min} = \min(Pr_b \text{ or } Pr_s)$	Miropolsky and Pikus [26], H_2O	46	65	78	86	37
$Nu_b = \begin{cases} 0.014 Re_b^{0.8} Pr_b^{0.8} (\bar{c}_p/c_{p,b})^{0.66} & \text{for } T_b < T_{pc} \\ 0.024 Re_b^{0.8} Pr_b^{0.8} (\bar{c}_p/c_{p,b}) & \text{for } T_{pc} < T_b \end{cases}$	Yamagata et al. [26], H_2O	9	12	15	18	168

Table 10 Summary of property data, uncertainty values, and sources used in analysis

Property	Temperature, K	Pressure, MPa	Uncertainty, %	Reference
Viscosity	<100	<35	0.5	[29,30,32]
	100–400	<35	4–15 ^a	[29,30,32]
	>400	<100	5	[33]
Density	$T_c \pm 1\%$	$(\rho_c \pm 20\%)$	greater, unknown	[29,30,32]
	liquid below T_c	<121	0.1	[29–31]
	gas below T_c	<Pc	0.25	[29–31]
	$T_c - 400$	0.005–121	0.2	[29–31]
	400–700	0.1–100	0.5	[33]
	700–3000	0.1–100	1	[33]
Specific heat (const. pressure)	$T_c \pm 5\%$	$(\rho_c \pm 30\%)$	6	[29–31]
	liquid below T_c	<121	3.0	[29–31]
	gas below T_c	—	2.0	[29–31]
	fluid above T_c , <400	0.05–121	3.0	[29–31]
	>400	0.01	0.02 ^a	[33]
	>400	35	3 ^a	[33]
Thermal conductivity	>400	100	8 ^a	[33]
	$T_c \pm 5\%$	$(\rho_c \pm 30\%)$	greater, unknown	[29–31]
	<100	<15	3	[29,30,32]
	<100	15–70.9	3–10 ^a	[29,30,32]
	100 < T < 400	-	10	[29,30,32]
	>400	-	7	[33]
	$T_c \pm 1\%$	$(\rho_c \pm 20\%)$	greater, unknown	[29,30,32]

^aWhere ranges of uncertainties are provided, a linear approximation is used to represent the uncertainty in the analysis.

modified Benedict–Webb–Rubin equation used by Younglove [31] cannot represent the proper behavior near the critical point, and is not considered to be valid in that region. Therefore, the uncertainty in the Nu correlation is not calculated near the critical region.

To determine the total uncertainty in Nu resulting from the uncertainties of each individual property variable, a general uncertainty analysis was performed. This was accomplished by using a Monte Carlo simulation program that was written in C++ (provided in [37]). Random errors were selected for each variable, based on a uniform parent population with σ equal to one-half of the assumed uncertainty for each variable at the particular temperature and pressure, specified in Table 10 [36]. A simulated measurement was produced by summing the drawn error with the assumed “true” value of the variable. The true value was determined through double interpolation between temperature and pressure for the particular transport property, obtained from tabulated data that is read into the program.

This process was performed for each variable, and the resulting Nu calculated at the specific temperature and pressure. This simulation was repeated 5000 times at each temperature and pressure with the resulting uncertainty in Nu determined as twice the calculated sample standard deviation [36]. The simulation was repeated for each combination of temperature and pressure within the range of interest. The uncertainties in experimentally measured variables (T , P , etc.) were not considered here.

As a representative case, the results of the uncertainty analysis for the Hess and Kunz [9] correlation are shown in Fig. 7. The black block on each plot is the near critical region where the uncertainties are not defined. In this region the resultant uncertainty is believed to be highest, but no reasonable estimate exists to quantify it precisely.

The McCarthy and Wolf [7] and Taylor [14] correlations, both based on bulk reference-type, produce comparable uncertainties. The uncertainty is lowest at approximately 1.8% under the liquid-vapor line, 2% for $T_R < 3$, and 5–7% for $3 < T_R < 12$. The Hendricks [8] correlation shows an uncertainty value of about 5.4% for $T_R < 2$, increasing to a maximum of 7% at higher temperatures. The Hess and Kunz [9] and Miller [10] correlation results reveal considerably higher uncertainties for these correlations at low pressures and temperatures and along the liquid-vapor line. The uncertainty is highest at approximately 10%, and is upward of 7–8% to $P_R = 2$. For higher temperatures, the uncertainty is similar to that of the Hendricks correlation at 5–7%.

Conclusions

A number of correlations have been published for heat transfer to supercritical hydrogen flowing turbulently in circular tubes. These correlations have been critically examined in this paper to characterize their range of validity. Comparison of the correlations with experimental heated tube data for supercritical hydrogen show

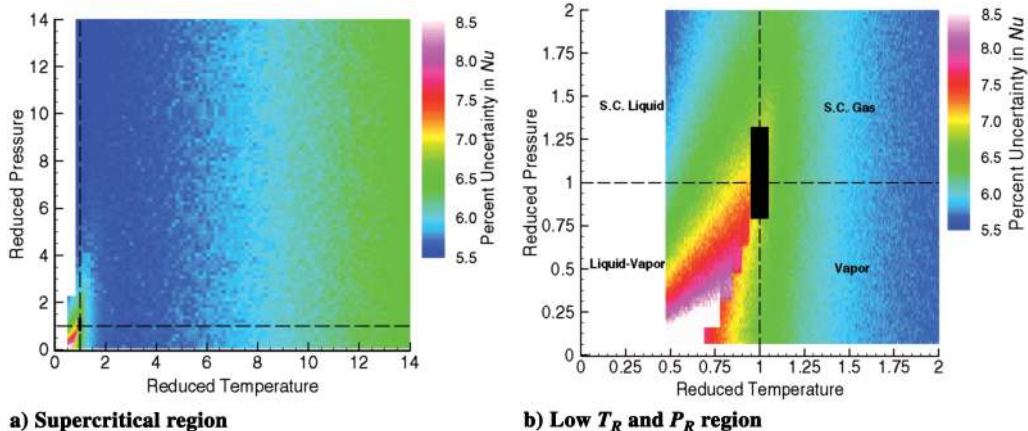


Fig. 7 Uncertainty associated with Hess and Kunz [6] correlation because of uncertainty in property data.

that the bulk reference-type correlations (McCarthy and Wolf, Taylor) overpredict the heat transfer near the critical points and around the pseudocritical temperature T^* line. This observation agrees with a purely analytical comparison of the correlations, in which the McCarthy and Wolf and Taylor predictions of the heat transfer coefficients spike near the T^* line, suggesting that this spike is actually an overprediction in this region and not a true representation of the heat transfer. The Hendricks and Taylor correlations underpredict along the T^* line. Hess and Kunz and Miller predict reasonably well along the T^* line, but both underpredict to the left of this line. The McCarthy and Wolf, Hendricks, Hess and Kunz, and Miller correlations all underpredict to varying degrees in the region of the transition from liquid to supercritical gas for $P_R > 4$. However, it is difficult to distinguish between the effects of thermally partially developed flow and the transition from liquid to supercritical gas, as this transition occurs at low x/D in the experimental data used in this analysis.

The integral property approach used in the Schacht and Quentmeyer correlation showed a good overall prediction of the experimental data (with a range of $\pm 56\%$ to cover 95% of the data), and performed better than other correlations in the low-temperature and low-pressure region. Using this reference-type with other forced convection heat transfer correlations could lead to improved predictions in this region, as well as accommodate the transition from liquid to supercritical gas and low x/D values. The Taylor correlation also showed good prediction for low x/D and reduced pressures above four.

A number of correlations proposed for variable property nonhydrogen supercritical fluids were evaluated for use with hydrogen. These correlations were compared with the compiled hydrogen heat transfer data sets. The correlations proposed by Miropolyski and Pikus, McAdams, Colburn, and Rohsenow all performed well with the hydrogen data (with ranges of ± 37 , ± 39 , ± 41 , $\pm 45\%$, respectively, to cover 95% of the data examined with $T_b \geq 50$ K). However, these are not significant improvements over the existing hydrogen correlations, all six of which predicted 95% of the data for $T_b \geq 50$ K between ± 40 and $\pm 45\%$. It is possible that modifying the exponents and constant coefficients of these correlation forms could provide better correlation with the hydrogen data.

The results of a detailed uncertainty analysis show that the uncertainty in Nu correlations for supercritical hydrogen as a result of uncertainty in property data ranges from about 1.8 to 10%. This uncertainty is affected by the reference temperature type used, with the bulk reference-type correlations having the lowest uncertainty in the low-pressure and low-temperature range. However, because this is lower than the errors observed in the correlation predictions, the property uncertainty does not appear to be a main contributor to the discrepancies in the prediction of the correlations.

Acknowledgments

This work was supported by NASA Grant NCC8-200 from NASA Marshall Space Flight Center with Mary Trawek as the NASA Contracting Officer's Technical Representative and Clark W. Hawk as Principal Investigator for the University of Alabama at Huntsville Propulsion Research Center. The authors would like to thank University of Alabama at Huntsville undergraduate research assistants Natalie Walker and Michelle Christensen for their support in compiling the experimental heat transfer data used in this paper.

References

- [1] Naraghi, M. H. N., *A Computer Code for Three-Dimensional Rocket Thermal Evaluation*, User Manual, Tara Technologies, New York, 2002.
- [2] Leahy, J. C., and Bates, L. L., "Features and Results Using P-Star: A Propulsion Sizing, Thermal, Accountability, and Weight Relationship First Order Modeling Tool," presented at 52nd JANNAF/1st Liquid Propulsion Subcommittee Meeting, JANNAF, May 2004.
- [3] Wennerberg, J. C., Anderson, W. E., Haberman, P. A., Jung, H., and Merkle, C. L., "Supercritical Flows in High Aspect Ratio Cooling Channels," AIAA Paper 2005-4302, 2005.
- [4] Sutton, G. P., and Biblarz, O., *Rocket Propulsion Elements*, 7th ed., Wiley, New York, 2001, pp. 197–240.
- [5] Huang, D. H., and Huzel, D. K., "Design of Liquid Propellant Rocket Engines," NASA SP-125, 1971.
- [6] Kakac, S., and Oskay, R., "Development of Two Layer Model Empirical Correlations for Variable Property Turbulent Forced Convection in Pipes," *Turbulent Forced Convection in Channels and Bundles: Theory and Applications to Heat Exchanges and Nuclear Reactors*, Vol. 2, edited by Kakac, S., and Spalding, D. B., Hemisphere, New York, 1979, pp. 563–611.
- [7] McCarthy, J. R., and Wolf, H., "Forced Convection Heat Transfer to Gaseous Hydrogen at High Heat Flux and High Pressure in a Smooth, Round, Electrically Heated Tube," *ARS Journal*, Vol. 30, April 1960, pp. 423–424.
- [8] Hendricks, R. C., Simoneau, R. J., and Friedman, R., "Heat-Transfer Characteristics of Cryogenic Hydrogen from 1000 to 2500 psia Flowing Upward in Uniformly Heated Straight Tubes," NASA TN-D-2977, 1965.
- [9] Hess, H. L., and Kunz, H. R., "A Study of Forced Convection Heat Transfer to Supercritical Hydrogen," *Journal of Heat Transfer*, Vol. 87, No. 2, 1965, pp. 41–48.
- [10] Miller, W. S., "Heat Transfer to Hydrogen Flowing Turbulently in Tubes," AIAA Paper 66-580, 1966.
- [11] Taylor, M. F., "A Method of Predicting Heat Transfer Coefficients in the Cooling Passages of NERVA and Phoebus-2 Rocket Nozzles," AIAA Paper 68-608, 1968.
- [12] Taylor, M. F., "Applications of Variable Property Heat-Transfer and Friction Equations to Rocket Nozzle Coolant Passages and Comparison with Nuclear Rocket Test Results," NASA TM-X-52793, 1970; also AIAA Paper 70-661, 1970.
- [13] Taylor, M. F., "Summary of Variable Property Heat-Transfer Equations and Their Applicability to a Nuclear Rocket Nozzle," NASA TM-X-52648, 1969.
- [14] Taylor, M. F., "Prediction of Friction and Heat-Transfer Coefficients with Large Variations in Fluid Properties," NASA TM-X-2145, 1970.
- [15] Schacht, R. L., and Quentmeyer, R. J., "Coolant-Side Heat-Transfer Rates for Hydrogen-Oxygen Rocket and a New Technique for Data Correlation," NASA TN D-7207, 1973.
- [16] Hines, W. S., McCarthy, J. R., Seader, J. D., and Trebes, T. M., "Investigation of Cooling Problems at High Chamber Pressures," Rocketdyne, Rept. No. R-3999, May 1963.
- [17] Seader, J. D., and Wagner, W. R., "Regenerative Cooling of Rocket Engines," *Chemical Engineering Progress Symposium Series*, Vol. 60, No. 52, 1964, pp. 130–150.
- [18] Thompson, W. R., and Geery, E. L., "Heat Transfer to Cryogenic Hydrogen at Supercritical Pressures," *Advances in Cryogenic Engineering*, Vol. 7, Jan. 1962, pp. 391–400.
- [19] Taylor, M. F., "Experimental Local Heat-Transfer and Average Friction Data for Hydrogen and Helium Flowing in a Tube at Surface Temperatures Up to 5600°R," NASA TN D-2280, 1964.
- [20] Taylor, M. F., "Experimental Local Heat-Transfer Data for Precooled Hydrogen and Helium at Surface Temperatures Up to 5300°R," NASA TN D-2595, 1965.
- [21] Taylor, M. F., "Correlation of Local Heat Transfer Coefficients for Single Phase Turbulent Flow of Hydrogen in Tubes with Temperature Ratios to 23," NASA TN-D-4332, 1968.
- [22] Miller, W. S., Seader, J. D., and Trebes, D., "Forced Convection Heat Transfer to Liquid Hydrogen at Supercritical Pressures," *Pure and Applied Cryogenics*, Vol. 4, Sec. 4, June 1965, pp. 173–191.
- [23] Hendricks, R. C., Graham, R. W., Hsu, Y. Y., and Friedman, R., "Experimental Heat-Transfer Results for Cryogenic Hydrogen Flowing in Tubes at Subcritical and Supercritical Pressures to 800 Pounds per Square Inch Absolute," NASA TN-D-3095, 1966.
- [24] Aerojet General Corp., "Heat Transfer to Cryogenic Hydrogen Flowing Turbulently in Straight and Curved Tubes at High Heat Fluxes," NASA CR-678, 1967.
- [25] Ghajar, A. J., and Strickland, D. T., "Forced and Mixed Convective Heat Transfer Correlations in the Laminar-Transition-Turbulent Regions for a Circular Tube with a Square-Edged Entrance," AIAA Paper 1990-1762, 1990.
- [26] Kakac, S., "The Effect of Temperature-Dependent Fluid Properties on Convective Heat Transfer," *Handbook of Single-Phase Convective Heat Transfer*, edited by Kakac, S., Shah, R. K., and Aung, W., Wiley, New York, 1987, pp. 18.1–18.56.
- [27] Jackson, J. D., and Hall, W. B., "Forced Convection Heat Transfer to Fluids at Supercritical Pressure," *Turbulent Forced Convection in Channels and Bundles: Theory and Applications to Heat Exchanges and Nuclear Reactors*, Vol. 2, edited by Kakac, S., and Spalding, D. B., Hemisphere, New York, 1979, pp. 563–611.

- [28] McCarthy, J. R., and Wolf, H., "The Heat Transfer Characteristics of Gaseous Hydrogen and Helium," Rocketdyne Div., North American Aviation, Rept. RR-60-12, Canoga Park, CA, Dec. 1960.
- [29] Lemmon, E. W., Peskin, A. P., McLinden, M. O., and Friend, D. G., *NIST 12: Thermodynamic and Transport Properties of Pure Fluids. NIST Standard Reference Database Number 12*, Version 5.0, National Institute of Standards and Technology, Boulder, CO, 2000.
- [30] Linstrom, P. J., and Mallard, W. G. (eds.), *NIST Chemistry WebBook, NIST Standard Reference Database Number 69*, National Institute of Standards and Technology, Gaithersburg, MD, June 2005, <http://webbook.nist.gov> [cited 18 Oct. 2005].
- [31] Younglove, B. A., "Thermophysical Properties of Fluids. I. Argon, Ethylene, Parahydrogen, Nitrogen, Nitrogen, Trifluoride, and Oxygen," *Journal of Physical and Chemical Reference Data*, Vol. 11, Suppl. 1, 1982, pp. 1-356.
- [32] McCarty, R. D., and Weber, L. A., "Thermophysical Properties of Parahydrogen from the Freezing Liquid Line to 5000°R for Pressures up to 10,000 psia," National Bureau of Standards TN 617, 1972.
- [33] McCarty, R. D., Hord, J., and Roder, H. M., "Selected Properties of Hydrogen (Engineering Design)," National Bureau of Standards, Monograph 168, 1981.
- [34] McCarty, R. D., "Hydrogen Technological Survey: Thermophysical Properties," NASA SP-3089, 1975.
- [35] Lach, J., Kielkiewicz, M., and Kosinski, M., "Heat Transport in Nuclear Reactor Channels," *Handbook of Heat and Mass Transfer, Vol. 1: Heat Transfer Operations*, edited by Chermishinoff, N. P., Gulf Publishing, Houston, TX, 1986.
- [36] Coleman, H. W., and Steele, W. G. *Experimentation and Uncertainty Analysis for Engineers*, 2nd ed., Wiley-Interscience, New York, 1999.
- [37] Locke, J. M., M.S. Thesis, Dept. of Mechanical and Aerospace Engineering, University of Alabama, Huntsville, AL, 2005.

J. Oefelein
Associate Editor